



Title	Photonic Bandgap Fiber Filter Design Based on Nonproximity Resonant Coupling Mechanism
Author(s)	Saitoh, Kunimasa; Florous, Nikolaos; Murao, Tadashi; Varshney, Shailendra; Koshiba, Masanori
Citation	IEEE Photonics Technology Letters, 19(19), 1547-1549 <a href="https://doi.org/10.1109/LPT.2007.903888">https://doi.org/10.1109/LPT.2007.903888</a>
Issue Date	2007-10-01
Doc URL	<a href="http://hdl.handle.net/2115/30229">http://hdl.handle.net/2115/30229</a>
Rights	©2007 IEEE. Personal use of this material is permitted. However, permission to reprint/republish this material for advertising or promotional purposes or for creating new collective works for resale or redistribution to servers or lists, or to reuse any copyrighted component of this work in other works must be obtained from the IEEE. IEEE, IEEE PHOTONICS TECHNOLOGY LETTERS, 19(19), 2007, pp.1547-1549
Type	article
File Information	IPTL19-19.pdf



[Instructions for use](#)

# Photonic Bandgap Fiber Filter Design Based on Nonproximity Resonant Coupling Mechanism

Kunimasa Saitoh, *Member, IEEE*, Nikolaos Florous, *Member, IEEE*, Tadashi Murao, Shailendra Varshney, *Member, IEEE*, and Masanori Koshiba, *Fellow, IEEE*

**Abstract**—The possibility of designing compact ultranarrow bandpass filters based on the phenomenon of nonproximity resonant tunneling in multicore photonic bandgap fibers is proposed and numerically demonstrated in this investigation by making use of versatile algorithms based on the finite-element method. The proposed multifunctional assembly exhibits bandpass transmission characteristics at four closed spaced wavelengths with a 3-dB bandwidth of about 1.2 nm and an insertion loss of about 0.8 dB. The isolation level between neighbor channels, ranging from 12 dB up to 15 dB, could be achieved at optical frequencies. The overall device performance offers some promising propagation characteristics for various all-fiber narrow bandpass filters.

**Index Terms**—Finite-element method (FEM), narrow bandpass filters, photonic bandgap fibers (PBGF).

## I. INTRODUCTION

THE extension of the concept of photonic crystals, from crystal lattices to fibers, resulted in the design of a hollow-core optical fiber that could trap light within, making it one of the candidates for realizing high-power transmission system and constructing novel optical fiber devices, in which the reproduction of the crystal lattice would be given by a periodic array of microscopic air holes that run along the entire fiber length. The considerable effort that has been undertaken in the last decade in the production of photonic crystal fibers (PCFs) [1], also known as microstructured optical fibers or holey fibers, led to the finding that glass capillaries could be stacked, fused together, and subsequently drawn to obtain the desired fiber structure. Although PCFs in their usual configuration are formed by a central defected region surrounded by multiple air holes arranged in various lattice configurations, recent advancements in manufacturing technology of PCFs such as the multiple-capillary drawing method [2], can readily realize multicore PCFs [3], [4].

One of the major challenges in the realization of all-fiber functional devices is the increasing number of operations that can be performed in a single fiber. Under such a scenario, the ultimate goal is to be able to fabricate in a single draw a complete all-fiber component provisioned on a preform level. Some

of the advantages of all-fiber devices are their simplified packaging, absence of subcomponent splicing losses, and environmental stability due to the absence of free-space optics. While the benefits of integrated all-fiber devices are significant enough to encourage the development of increasingly complex components, the major drawback regarding their practical realization is the unavoidable complexity of the required transverse refractive index profile.

All the above mentioned challenges can be, in a certain degree, utilized by using a novel class of photonic bandgap fiber (PBGF) coupler that was recently introduced [5], which operates by resonant rather than proximity coupling [6], where the energy transfer is realized via transverse resonators integrated into the fiber's cross section. Perhaps the main advantage of this coupling mechanism is its inherent scalability as additional fiber cores could be integrated into the existing fiber cross section simply by placing them far enough from the existing circuitry to avoid proximity crosstalk, and then making the necessary intercore connections with various transverse light "architectures" in a direct analogy to the "on chip electronics integration."

Taking all the above circumstances into account, we devote the present investigation to generalize the idea behind the resonant tunneling effect in multicore PBGF assemblies by proposing and numerically verify the performance of a novel all-fiber coupling system with multiple integrated resonators in its profile. Through versatile algorithms for efficient modal [7] and beam propagation [8] characterization based on the finite-element method (FEM), we theoretically investigate the mutual coupling mechanism occurring in multicore PBGFs, which lead to the realization of efficient ultranarrow bandpass filters.

## II. DEVICE CONCEPT AND DEFINITIONS

The schematic representation of the proposed multicore PBGF is depicted in Fig. 1. The hollow cores are formed in a silica-based PBGF with a cladding refractive index  $n = 1.45$ , by removing seven air holes and smoothing the resulting core edges. The pitch constant is chosen to be  $\Lambda = 2 \mu\text{m}$ , while the normalized diameter of the air holes in the cladding of the fiber is  $d/\Lambda = 0.9$ , with a total number of 14 hole layers in the cladding. The fundamental bandgap, where the core guided modes are found, extends between  $1.29 \mu\text{m} < \lambda < 1.40 \mu\text{m}$  [9]. The formation of a multicore coupler, operating at four distinct wavelengths, can be achieved by placing hollow cores of  $8\Lambda$  apart from each other, counting from the center of each core along the x-axis (horizontal axis), while  $4\sqrt{3}\Lambda$  apart from each other along the y-axis (vertical axis). In this case, four dissimilar high-index transverse resonators having normalized

Manuscript received March 7, 2007; revised May 26, 2007.

The authors are with the Division of Media and Network Technologies, Hokkaido University, Sapporo 060-0814, Japan (e-mail: ksaitoh@ist.hokudai.ac.jp).

Color versions of one or more of the figures in this letter are available online at <http://ieeexplore.ieee.org>.

Digital Object Identifier 10.1109/LPT.2007.903888

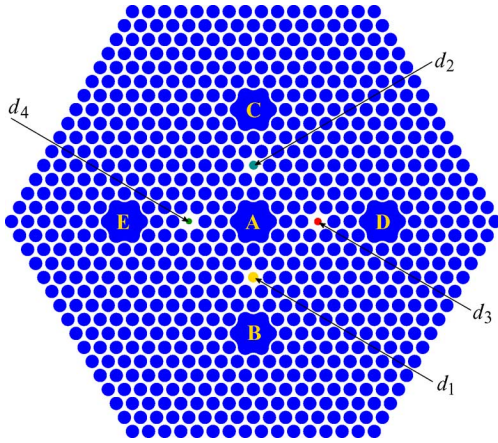


Fig. 1. Schematic cross section of the proposed five-core multifunctional PBGF assembly utilizing a nonproximity resonant tunneling effect. As an input core, we consider the central core *A*, while *B*, *C*, *D*, and *E* are the output cores which are coupled to the input core *A* via four dissimilar transverse resonators with normalized diameters  $d_1/\Lambda$  (yellow),  $d_2/\Lambda$  (cyan),  $d_3/\Lambda$  (red), and  $d_4/\Lambda$  (green).

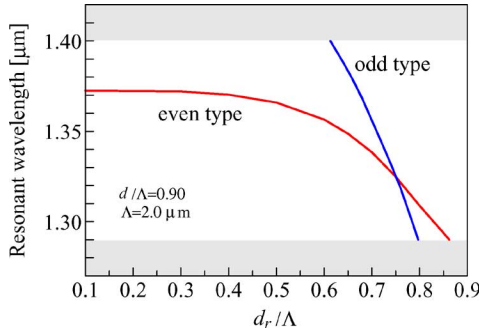


Fig. 2. Evaluation of the resonant wavelength (micrometers) of the odd-type excited resonant mode (blue solid curve), as well as the even-type excited resonant modes (red solid curve), as a function of the normalized resonator's diameter  $d_r/\Lambda$ .

air-hole diameters  $d_1/\Lambda$  (yellow),  $d_2/\Lambda$  (cyan),  $d_3/\Lambda$  (red), and  $d_4/\Lambda$  (green), are integrated into the fiber's profile by reducing (high-index defects) the diameters of the air holes in the middle of the line joining the cores. This multicore coupler is a generalization of the device initially proposed in [5]. The fiber structure dealt in [5] has three cores separated by two resonators and these resonators are placed in horizontal directions. If we introduce multicores in vertical directions as well as horizontal directions, the design procedure is more complicated and the polarization state and the fiber length have to be carefully selected.

### III. NUMERICAL RESULTS AND DEVICE PERFORMANCE

For this PBGF structure, by using an accurate modal analysis based on a full-vector FEM solver [7], in Fig. 2 we evaluate the resonant wavelength for the two types of resonant modes, namely the odd-type excited resonant mode (odd pattern along the horizontal axis, blue solid curve), as well as the even-type excited resonant mode (even pattern along the horizontal axis, red curve), as a function of the normalized resonator's diameter  $d_r/\Lambda$ . It is clear that, for the resonant modes localized in the

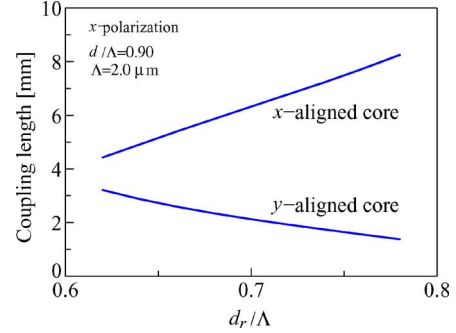


Fig. 3. Calculated coupling length (in millimeters) of the *x*-polarized state as a function of the normalized resonator's diameter  $d_r/\Lambda$ , for the *x*-aligned core and the *y*-aligned core.

high index defect, there is no polarization dependence due to the six-fold symmetry of the structure, however, for the dual-core coupler coupled with resonator such as cores *A* and *B* or cores *A* and *D*, there is a strong polarization dependence due to the lack of six-fold symmetry. The odd-type resonant mode can be coupled to the fundamental *x*-polarized (horizontally polarized) hollow-core mode, while the even-type resonant mode can be coupled to the fundamental *y*-polarized (vertically polarized) hollow-core mode. Therefore, we plotted both the odd-type and even-type resonant modes in Fig. 2. It is evident that possible values of the resonator's diameters are in the range of  $0.62 < d_r/\Lambda < 0.8$  for the *x*-polarized hollow-core mode coupled with the odd-type resonant mode, while  $0 < d_r/\Lambda < 0.86$  for the *y*-polarized hollow-core mode coupled with the even-type resonant mode. This practically means that by appropriately setting the resonator's diameter  $d_r/\Lambda$ , we can achieve a predetermined resonance at different wavelengths inside the bandgap region of the PBGF. In such a case, the coupling lengths of the proposed coupler for complete power transfer from central core to another one through resonant coupling effect are plotted (in millimeters) as a function of the normalized resonator's diameter  $d_r/\Lambda$  in Fig. 3 for the *x*-polarization, and Fig. 4 for the *y*-polarization, respectively, calculated using a FEM modal solver. The coupling length can be calculated through the supermode analysis of the "three-core" directional coupler (that is the system composed of two hollow cores and one resonator) [5]. From these results, we can clearly see that the coupling length characteristics corresponding to the two different polarizations are essentially different, because the resonant state coupled with the *x*-polarized hollow-core mode has an odd-type profile along the horizontal axis, while the resonant state coupled with the *y*-polarized hollow-core mode has an even-type profile along the horizontal axis which is significantly different from the odd-type resonant mode. For the *y*-polarization, we can conclude that the coupling lengths for the *x*-aligned core system (cores *A* and *D*, or *A* and *E*) as well as for the *y*-aligned core-system (cores *A* and *B*, or *A* and *C*) can exhibit a common coupling length of about 3 mm, a very crucial observation which makes the *y*-polarized operation of this fiber assembly more appropriate. Therefore, we can determine that the appropriate normalized resonators' diameters are  $d_1/\Lambda = 0.82$ ,  $d_2/\Lambda = 0.80$ ,  $d_3/\Lambda = 0.76$ , and  $d_4/\Lambda = 0.73$  for the *y*-polarization.

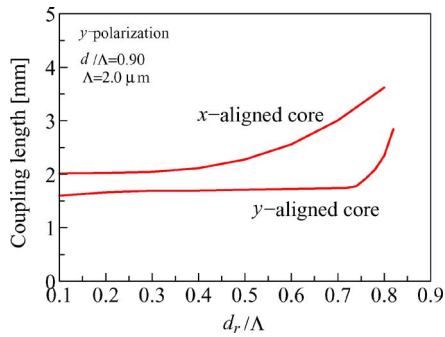


Fig. 4. Calculated coupling length (in millimeters) of the  $y$ -polarized state as a function of the normalized resonator's diameter  $d_r/\Lambda$ , for the  $x$ -aligned core and the  $y$ -aligned core.

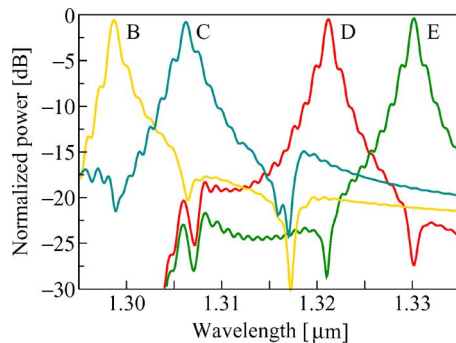


Fig. 5. BPM simulation result of transmission characteristics as a function of the operating wavelength at the four different output cores,  $B$  (yellow curve),  $C$  (cyan curve),  $D$  (red curve), and  $E$  (green curve), and for the optimized design parameters,  $L = 3$  mm,  $\Lambda = 2$   $\mu\text{m}$ ,  $d/\Lambda = 0.9$ ,  $d_1/\Lambda = 0.82$ ,  $d_2/\Lambda = 0.80$ ,  $d_3/\Lambda = 0.76$ , and  $d_4/\Lambda = 0.73$ .

The transmission characteristics of the proposed PBGF structure for the  $y$ -polarized state are shown in Fig. 5. It is worth mentioning that in this case and due to the fact that the overall cross section of the proposed fiber does not exhibit any symmetry, the whole fiber had to be discretized and analyzed, a fact that reveals the high complexity of the calculation. Here the  $y$ -polarized (vertically polarized) fundamental mode was launched into the input core  $A$  (central core) and the output powers from cores  $B$ ,  $C$ ,  $D$ , and  $E$  with a total fiber length of  $L = 3$  mm were calculated using a full-vector beam propagation method (BPM) algorithm [8]. From these results, we can clearly observe that the proposed multifunctional PBGF structure exhibits a narrow bandpass transmission characteristics at four distinct closed-spaced wavelengths, namely  $\lambda_1 = 1.299$   $\mu\text{m}$  (core  $B$ ),  $\lambda_2 = 1.306$   $\mu\text{m}$  (core  $C$ ),  $\lambda_3 = 1.321$   $\mu\text{m}$  (core  $D$ ), and  $\lambda_4 = 1.330$   $\mu\text{m}$  (core  $E$ ); all of them have a 3-dB bandwidth of about 1.2 nm and a corresponding insertion loss of about 0.8 dB. The insertion loss is due to the coupling length difference corresponding to different resonators. In this case, an isolation level ranged between 12 dB (for the  $y$ -aligned cores  $B$  and  $C$ ) up to 15 dB (for the  $x$ -aligned cores  $E$  and  $D$ ) could be achieved. We

can control the isolation level by varying the cladding air-hole diameter. These transmission characteristics are quite promising for applications such as resonant sensing platforms or narrow bandpass filtering. The suppression of the sidelobes in comparison to previous reported filters based on conventional fiber technology as well as the ultranarrowband response and the reasonable short coupling length are the main advantages of the proposed PBGF architecture. The feasibility of our proposed fiber may be somehow difficult in the present stage of technology, but we strongly believe that with more advanced fabrication technologies that will be introduced in the near future, the realization of the proposed fiber device will become possible, thus advancing the application areas of PBGFs.

#### IV. CONCLUSION

To conclude our investigation, we have proposed and numerically verified the propagation characteristics of a novel bandpass filter based on the resonant tunneling phenomenon in a five-core PBGF. The resonant tunneling effect in multicore PBGFs was successfully utilized to construct multifunctional all-fiber system assemblies for filtering and sensing applications. Based on the prescribed technology, certain types of fluidic and biochemical sensors, whose operation will be based on the infiltration of highly thermoresponsive substances [10] into the proposed PBGF device are currently under investigation.

#### REFERENCES

- [1] P. St. J. Russell, "Photonic crystal fibers," *Science*, vol. 299, pp. 358–362, Jan. 2003.
- [2] S. Kawanishi, T. Yamamoto, H. Kubota, M. Tanaka, and S. Yamaguchi, "Dispersion controlled and polarization maintaining photonic crystal fibers for high performance network systems," *IEICE Trans. Electron.*, vol. E87-C, pp. 336–342, Mar. 2004.
- [3] B. J. Mangan, J. C. Knight, T. A. Birks, P. St. J. Russell, and A. H. Greenaway, "Experimental study of dual-core photonic crystal fibre," *Electron. Lett.*, vol. 36, pp. 1358–1359, Aug. 2000.
- [4] W. N. MacPherson, J. D. C. Jones, B. J. Mangan, J. C. Knight, and P. St. J. Russell, "Two-core photonic crystal fiber for Doppler difference velocimetry," *Opt. Commun.*, vol. 233, pp. 375–380, Aug. 2003.
- [5] N. J. Florous, K. Saitoh, T. Murao, M. Koshiba, and M. Skorobogatiy, "Non-proximity resonant tunneling in multi-core photonic bandgap fibers: An efficient mechanism for engineering highly-selective ultra-narrow bandpass splitters," *Opt. Express*, vol. 14, pp. 4861–4872, May 2006.
- [6] J. Lægsgaard, "Directional coupling in twin-core photonic bandgap fibers," *Opt. Lett.*, vol. 30, pp. 3281–3283, Dec. 2005.
- [7] K. Saitoh and M. Koshiba, "Full-vectorial imaginary-distance beam propagation method based on a finite element scheme: Application to photonic crystal fibers," *IEEE J. Quantum Electron.*, vol. 38, no. 7, pp. 927–933, Jul. 2002.
- [8] K. Saitoh and M. Koshiba, "Full-vectorial finite element beam propagation method with perfectly matched layers for anisotropic optical waveguides," *J. Lightw. Technol.*, vol. 19, no. 3, pp. 405–413, Mar. 2001.
- [9] K. Saitoh and M. Koshiba, "Leakage loss and group velocity dispersion in air-core photonic bandgap fibers," *Opt. Express*, vol. 11, pp. 3100–3109, Nov. 2003.
- [10] K. Saitoh, N. J. Florous, S. K. Varshney, and M. Koshiba, "Tunable photonic crystal fiber couplers infiltrated with highly-thermo-responsive liquid crystal substances," presented at the CLEO/QELS, Baltimore, MD, May 2007, Paper CTu117.